

Support information

Single-Cell Resolution Diagnosis of Cancer cells by Carbon Nanotube Electrical Spectroscopy

M. Abdolahad¹, M. Janmaleki², M. Taghinejad¹, H. Taghnejad¹ and S. Mohajerzadeh^{1*}

¹Nano-Electronics center of excellence., School of Electrical and Computer Engineering, University of Tehran, P.O. Box 14395/515, Tehran, Iran

²Medical Nanotechnology and Tissue Engineering Research Center, Shahid Beheshti University of Medical Science P.O. Box 1985717443Tehran, Iran

*Email : mohajer@ut.ac.ir

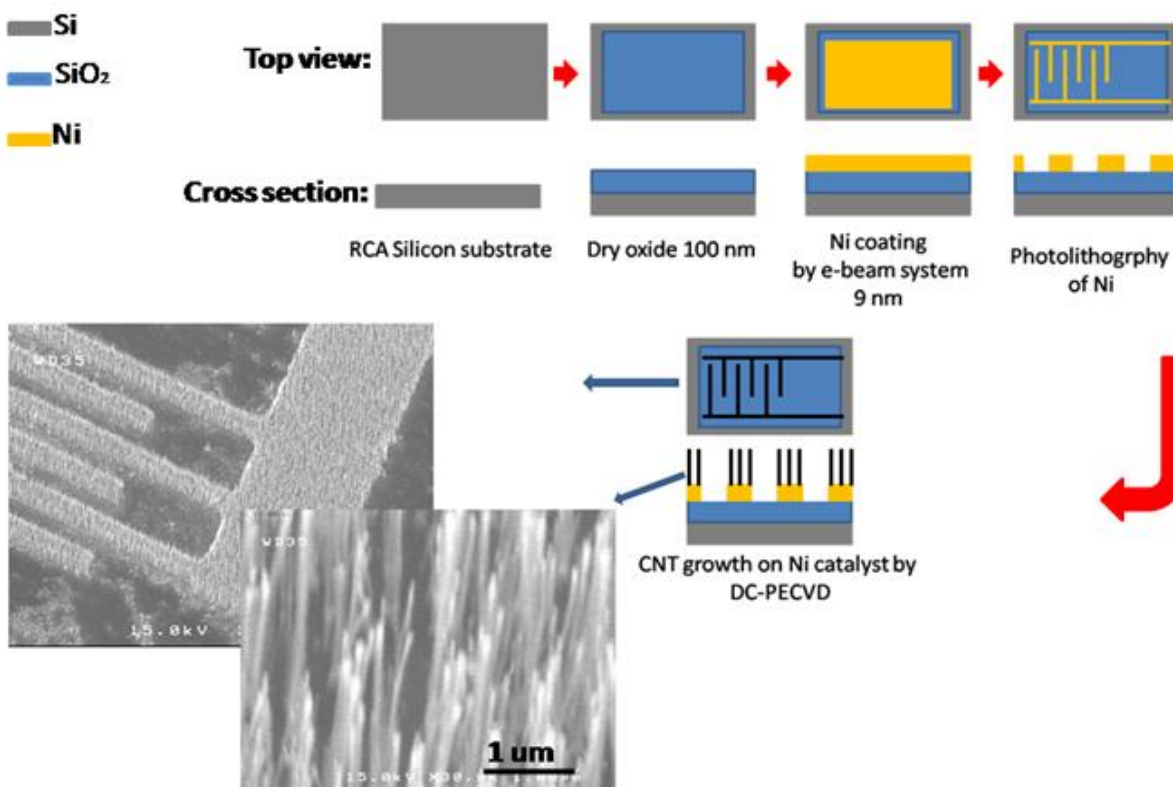


Figure S1. Fabrication process of CNT based electrical spectroscopy system. First the Si substrate was cleaned by RCA procedure, subsequently the SiO₂ layer has been grown on the substrate using dry oxide

furnace at a temperature of 1050°C. Then the Ni catalyst layer with the thickness of 9 nm was coated on the surface by e-beam coating system. In the next step, the Ni layer has been patterned using standard photo-lithographically and the interdigital arrays (IDA) are formed on the surface. Finally, the vertically aligned carbon nanotubes were grown on patterned regions by Direct Current Plasma Enhanced Chemical Vapor Deposition (DC-PECVD) with the assistance of acetylene (C_2H_2), H_2 and O_2 as well as a plasma current of 38 mA.

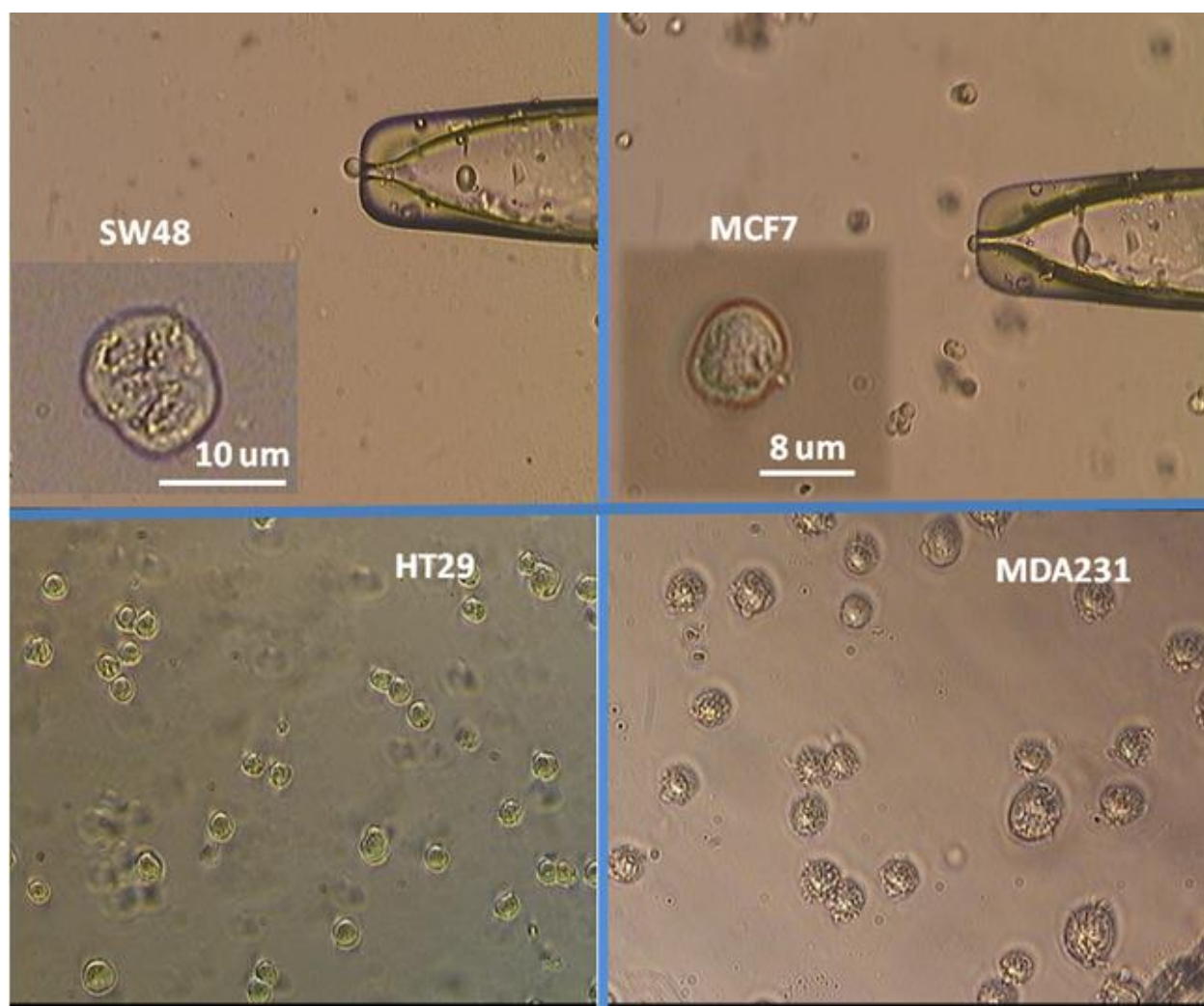


Figure S2. Optical microscopy images of colon and breast cancer cells prepared for testing in cancer electrical analysis system.

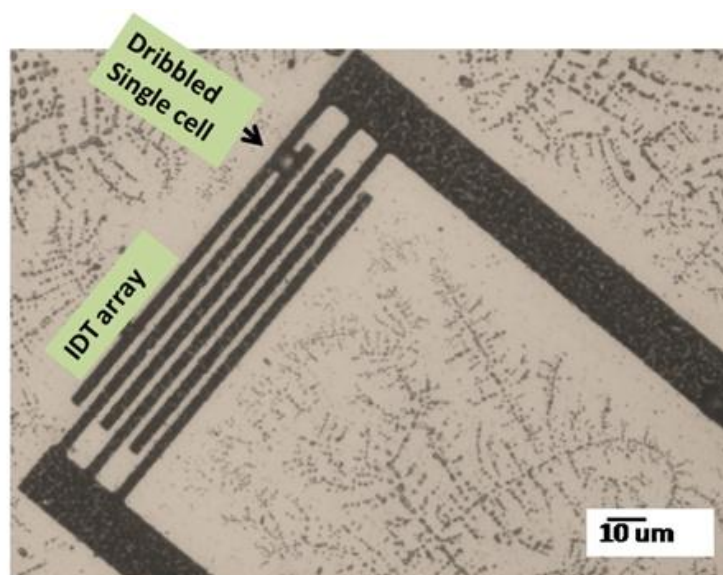


Figure S3. Optical microscopy image of a cancer cell (MCF7) dribbled between IDA of CNT endoscope. Immediately after dropping by micropipette.

Cell viability during signal extraction by CNT electrodes

Singhal *et al.* report a stable live state for the cell after CNT penetration through its membrane and inner parts for a long period of time¹. Moreover, insertion of vertically aligned nanotubes with their fine diameter and uniform geometry into the inner parts of the cell does not induce any membrane rupture under the experimental conditions required for the direct electrical studies (Figure 2-b of the main paper).

Also for more corroboration, the cancer cell was tagged with green fluorescent protein (GFP) before locating between nano electrodes. Figure S4-a presents the fluorescent microscopy image from the entrapped cancer cell which has been tagged by GFP on vertically aligned CNT arrays. The expression of GFP in this image confirms the living state of the cell after the penetration of CNT tips into its membrane. Figure S4-b shows a live HT29 cell on CNT cancer endoscope biosensor during signal extraction from the cell membrane, as observed in figure 2-a.

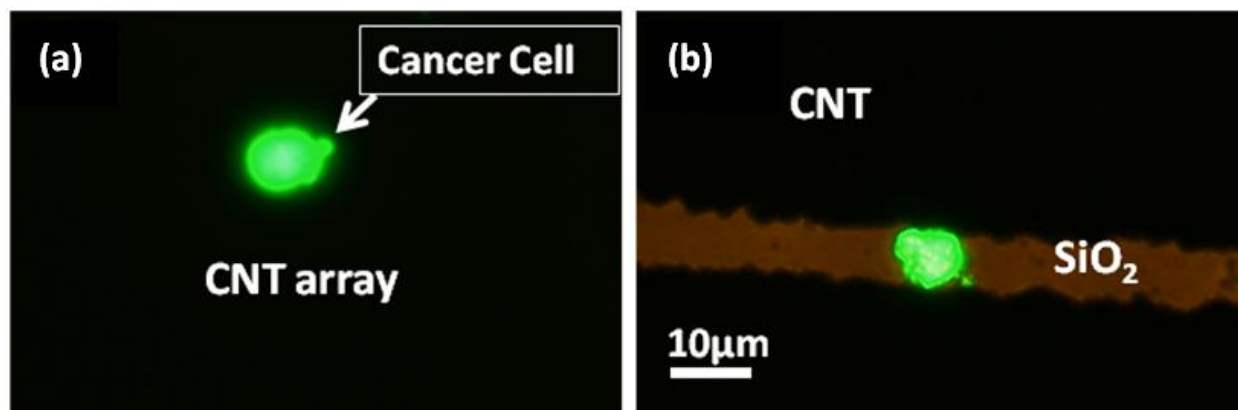


Figure S4. (a) A fluorescent image of a living HT29 cell trapped on CNT arrays expressing a GFP-tagged nuclear body protein (green). (b) Fluorescent image of the cell dribbled between CNT cancer endoscope nano-electrodes during signal extraction.

Electrical Resonance of the cell and its degradation during cancer progression

As known, the dimension of the electrical impedance is $ML^2T^3A^{-2}$ which M , L , T and A refer to mass, length, time and electrical current units respectively. Also the dimension of frequency is T^{-1} . The second derivative of impedance vs. frequency has a dimension of $ML^2A^{-2}T^{-4}$ which is the same as the dimension of electrical conductance (G). As in some frequencies the conductance of the cell sharply rises (figures 3-c, 3-d, 4-c and 4-d of the paper), this diagram may highly be correlated with the action potential (the intrinsic electrical activity of cells) as well as electrical resonance of the cell in particular frequencies in which the conductance of the cell suddenly increases².

The reason behind the drop in the cancer cell electrical resonance is based on the depolarization. The decrease of the bioelectronics potential of cancer cells, due to a defect of the cytochrome a/a3, namely the cytochrome oxidase, is caused by a carcinogen effect³⁻⁵. It means that the

erasure of cell vibrancy and resonance are based on a disorder of the cellular respiration which leads to destruction of the respiratory chain (especially of cytochrome oxidase) and results in the potential drop and the depolarization of the cell. As a result, cancer cells do not vibrate with the normal cell formation anymore⁶⁻⁷

Cell membrane Ion channel disruption during carcinogenesis

Cancerous transformation leads to abnormalities in ion permeability of cell membrane. This is a discernible disruption in the impedance value of the cell after metastatic progression. This variation might result in the disruption of the cell membrane ion channels such as more Na-ion accumulation inside the cell while K-ions diffuse outside⁸ which supports the further impedance disruption of high cancerous transformed cell in comparison with lower one (Figure S5).

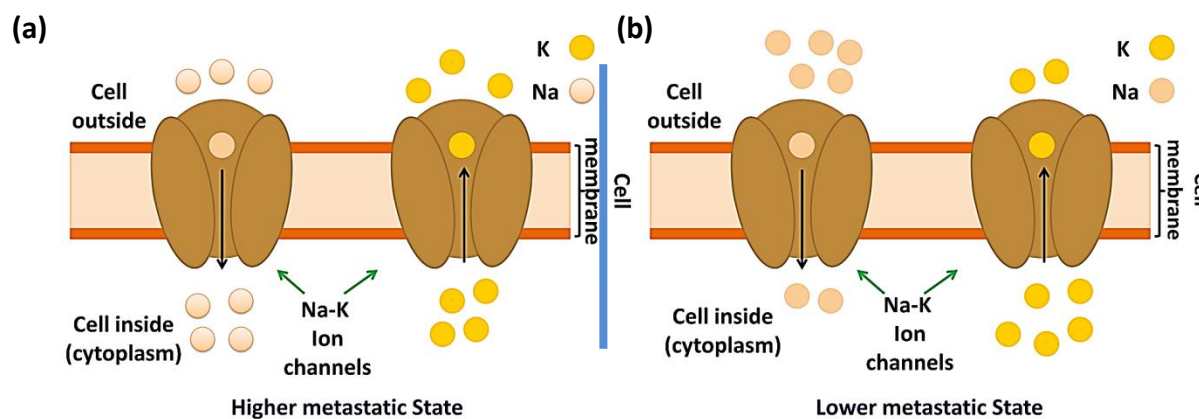


Figure S5. Schematic drawing from cell membrane ion permeability increment after metastatic progression, which relates to Na accumulation inside and K penetration outside the cell membrane as

described in the schematic drawings of (a) high metastatic and (b) primary stages of cancer cell membrane respectively.

CNT entrance to cell inner parts

CNT penetration to cell inner parts (such as nuclei) may lead to two effects: first, cell viability and second, signal extracted from the endoscope. For the former case it must be borne in mind that our previously reported viability tests (MTT and LDH⁹) as well as GFP results presented in this paper show that the CNT penetrated cells were completely alive. On the other hand, in this experiment we do not flow the cell on the tube and it has just been dribbled between two CNT covered electrodes, so the weight of the cell is assumed to be the main force of CNT penetration to the cell. Recently we reported¹⁰, that the cell traction force (CTF) applied on nanotubes after their entrapment is related to CNT deflection angle. In our CNT-endoscope the deflection angle of the tubes is much lower than the nanotubes involved in the entrapment of flown cells as shown in figure S6. It is observed in figure S6-a and b that the CNTs enter the inner parts of the cell. But the nanotubes in CNT-endoscope (S6-c) are not largely deflected nor enter the cell inner parts or reach the nuclei. So as the weight force of the cell is much lower than cell CTF¹⁰, the nanotube of CNT-endoscope may just enter the membrane of the cell.

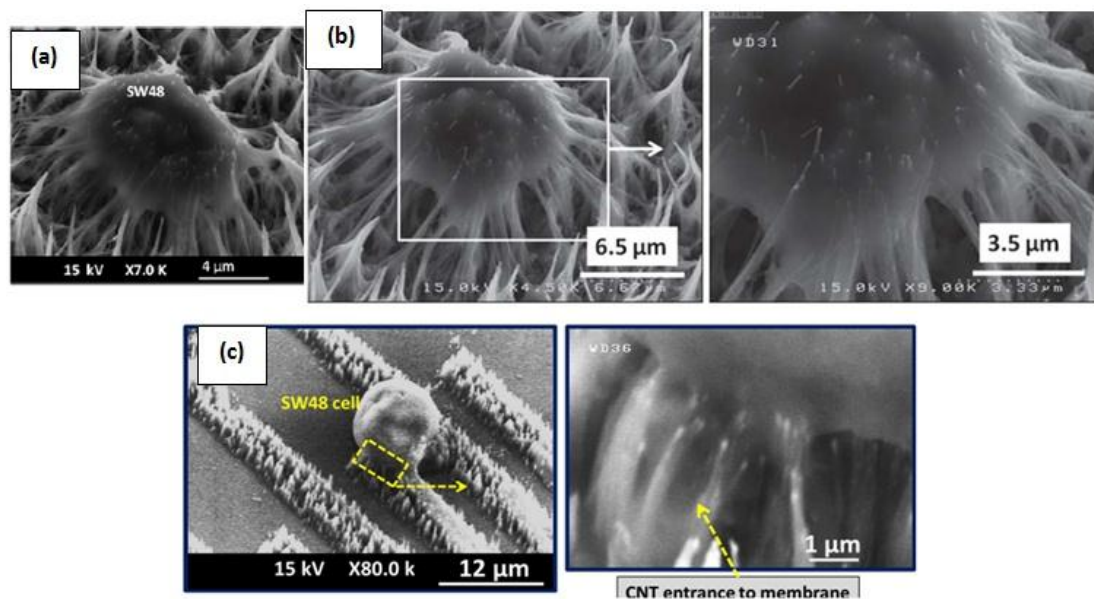


Figure S6. The comparative SEM images of SW48 cancer cell (a) entrapped on CNT arrays for cell traction force (CTF) measurement [10] (b) entrapped on CNT-ECIS [9]. (c) Dribbled on CNT-endoscope (present work). It is observable that the CNT penetration depth in CNT endoscope is considerably shorter than other ones and nanotubes just enter the cell membrane.

These results somehow solve the second concern about signal extraction from the cell. As we have calculated from the equal circuit model (figure 5 of the main paper), the membrane has a key role in the impedance signal of the cell in all ranges of frequencies even if the CNTs penetrate to the nuclei of the cell. It has been shown that the signals extracted from CNT-endoscope depend on the membrane electrical fluctuations. This is originated from the conductivity and dielectric differences between membrane and inner parts of the cell (cytoplasm and nuclei) as well as the geometry of CNT electrodes penetrated to the cell. So, the nuclei might not have an important effect on the response of CNT endoscope.

Single cell extreme drug resistance (EDR) assay with CNT electrical spectroscopy

Cell incubation procedure with Triton: We have cultured four separate samples of the HT29 cancer cells in the same manner as mentioned above. Here, we add 1%, 5% and 25% wt of Triton X-100 (a cell necrotic agent produced in Merck Co, Germany) to the media solution of three separated cell samples for 3 minutes. Then the drug added solution was removed and a fresh media solution was replaced. The electrical measurement was experimented for both control and Triton treated samples.

Cell incubation procedure with Paclitaxel:

Three separate samples of the HT29 cancer cells were cultured and Subsequently, 0.6 and 2.0 μmolar of paclitaxel (Drug for epithelial carcinoma destruction with molecular formula: $\text{C}_{47}\text{H}_{51}\text{NO}_{14}$ produced in Xi'an Hao-xuan Bio-tech Co., Ltd) were added to the media solution of two separated cell samples and the drugs were incubated with the cells for 48 hrs in incubator. Then the drug added solution was removed and a fresh media solution was replaced. The electrical characteristics were measured for both control and drug treated samples.

EDR is an advanced laboratory test for cancer metastatic detection also known as, chemotherapy drug resistance test. The original EDR is performed by growing a portion of the cancer tumor in the presence of different chemotherapy drugs in the laboratory¹¹⁻¹². If the cancer cells grow in the presence of a very high dosage of a chemotherapy drug, the cancer is less unlikely to respond to that specific drug within the patient's body. CNT cancer spectroscopy system could precisely

detect the resistance of the single cancer cell to drug (after controlled incubation of cell with drugs under known doses and times) by signal extraction from the cell membrane. The anti cancer drugs are categorized depending on the level of their destroying mechanism of cancerous cells. Some of these drugs will turn the state of the cancer cell into a necrosis. Necrotic cells swell and their plasma membrane eventually ruptures¹³, so the impedance of its membrane will be dropped. Other types of such drugs raze the cancerous cells by slowing or stopping them from dividing and growing which turn the state of the cells to apoptosis depending on the tumoral stage of the cell as well as the strength of the drug¹⁴. In addition, the electrical response of the live cell membrane becomes lower during apoptosis¹⁵. Here, we investigated the EDR of single HT29 cell to anti-cancer agents from two groups named as Triton X-100 and Paclitaxel¹⁶ (Drug for epithelial cancer destruction) by means of our device. The resistance of HT29 cell to various doses and incubation times of paclitaxel and triton was investigated. To investigate HT29 single cell EDR assay with Paclitaxel, we incubated the HT29 cells with 2.0 and 0.6 μ molar solution of Paclitaxel for 48 hrs separately in a manner mentioned in experimental section. The cell membrane impedance measurements were carried out on each treated cell using the same procedure as mentioned above.

Figure S7-a presents the impedance frequency diagram of HT29 cell incubated with different doses of paclitaxel. The HT29 cell membrane impedance at 20 kHz reduced from 230 to 61 and 49 Ω by incubation in 0.6 and 2.0 μ molar concentration of paclitaxel, respectively. A significant reduction in the cell membrane impedance by a little increase in the dose of paclitaxel shows the accuracy of our CNT-based cancer cell electrical analysis for EDR assay. In another study, the cell was incubated with 25%, 5% and 1% wt of triton for 3 min. The diagrams of figure S7-b show that the impedance of HT29 cell starts to be disrupted when the dose of triton is increased.

The HT29 cell membrane impedance at 20 kHz reduces from 230 to 70, 68 and 65 Ω by incubation in 1%, 5% and 25% wt of triton, respectively. An increment in the percentage of added triton to cell culture media resulted in a noticeable disruption of HT29 impedance, which could be related to the necrosis state of the cell.

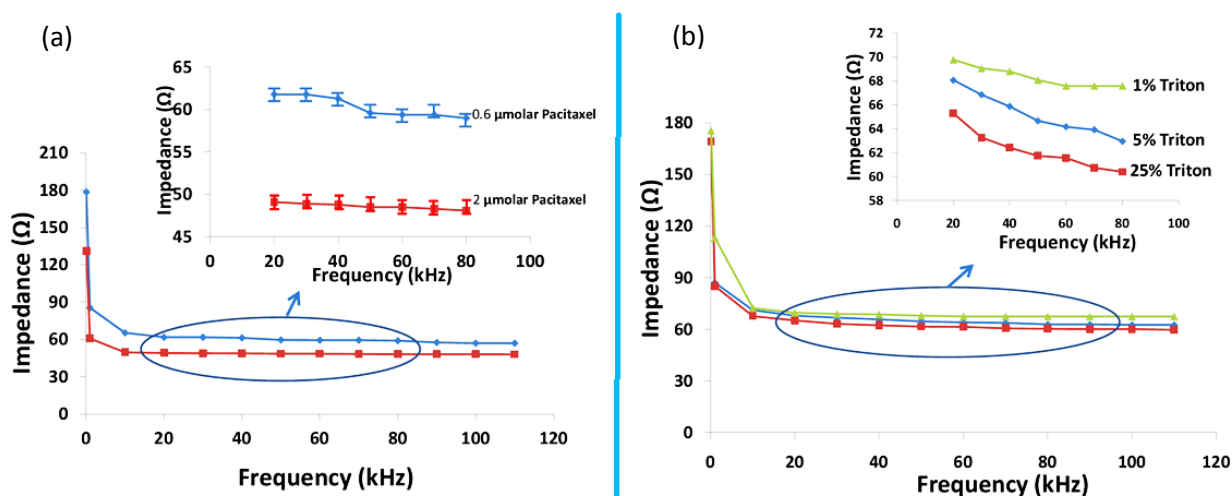


Figure S7. (a) Impedance diagram of HT29 single cell treated with 0.6 and 2.0 μ molar of paclitaxel at different frequencies measured by CNT based cancer spectroscopy of single cell resolution EDR assay. The impedance diagram of untreated sample has been previously presented in figure 4. (b) Impedance diagram of HT29 single cell treated with 1%, 5% and 25% of triton at different frequencies measured by this tool. An increment in the dose of Triton result in observable decrement in treated cell impedance.

References

1. Singhal, R.; Orynbayeva, Z.; Kalyana Sundaram, R. V.; Niu, J. J.; Bhattacharyya, S.; Vitol, E. A.; Schrlau, M. G.; Papazoglou, E. S.; Friedman, G.; Gogotsi, Y., Multifunctional carbon-nanotube cellular endoscopes. *Nat Nano* 2011, 6 (1), 57-64.
2. Dubois, M. L., *Action Potential: Biophysical and Cellular Context, Initiation, Phases and Propagation*. Nova Science Pub Inc: 2010.

3. Charman, R., Electrical Properties of Cells and Tissues. In Clayton's electrotherapy, Kitchen, S.; Bazin, S., Eds. Saunders: 1996.
4. Kirson, E. D.; Gurvich, Z.; Schneiderman, R.; Dekel, E.; Itzhaki, A.; Wasserman, Y.; Schatzberger, R.; Palti, Y., Disruption of cancer cell replication by alternating electric fields. *Cancer Res* 2004, 64 (9), 3288-95.
5. Zimmermann, U.; Vienken, J.; Pilwat, G., Rotation of cells in an alternating electric field: the occurrence of a resonance frequency. *Z Naturforsch C* 1981, 36 (1-2), 173-7.
6. Stern, R. G.; Milestone, B. N.; Gatenby, R. A., Carcinogenesis and the plasma membrane. *Medical Hypotheses* 1999, 52 (5), 367-372.
7. Tarantola, M.; Marel, A. K.; Sunnick, E.; Adam, H.; Wegener, J.; Janshoff, A., Dynamics of human cancer cell lines monitored by electrical and acoustic fluctuation analysis. *Integr Biol (Camb)* 2010, 2 (2-3), 139-50.
8. Kunzelmann, K., Ion channels and cancer. *J Membr Biol.* 2005,205(3):159-73.
9. Abdolahad, M.; Taghinejad, M.; Taghinejad, H.; Janmaleki, M.; Mohajerzadeh, S., A vertically aligned carbon nanotube-based impedance sensing biosensor for rapid and high sensitive detection of cancer cells. *Lab on a Chip* 2012, 12 (6), 1183-1190.
- 10.** Abdolahad, Mohajerzadeh, S, M.; Janmaleki, M. Taghinejad, H.; Taghinejad, M.; Evaluation of the shear force of single cancer cells by vertically aligned carbon nanotubes suitable for metastasis diagnosis†; *Integrative Biology*, 2013, DOI: 10.1039/c2ib20215h
11. Matsuo, K.; Eno, M. L.; Im, D. D.; Rosenshein, N. B.; Sood, A. K., Clinical relevance of extent of extreme drug resistance in epithelial ovarian carcinoma. *Gynecologic Oncology* 2010, 116 (1), 61-65.
12. Callaghan, R.; van Gorkom, L. C. M.; Epanand, R. M., A comparison of membrane properties and composition between cell lines selected and transfected for multi-drug resistance. *Br J Cancer* 1992, 66 (5), 781-786.
13. Lee, R. M.; Choi, H.; Shin, J.-S.; Kim, K.; Yoo, K.-H., Distinguishing between apoptosis and necrosis using a capacitance sensor. *Biosensors and Bioelectronics* 2009, 24 (8), 2586-2591.
14. Liang, N.; Sun, S.; Li, X.; Piao, H.; Piao, H.; Cui, F.; Fang, L., α -Tocopherol succinate-modified chitosan as a micellar delivery system for paclitaxel: Preparation, characterization and in vitro/in vivo evaluations. *International Journal of Pharmaceutics* 2012, 423 (2), 480-488.

15. Arndt, S.; Seebach, J.; Psathaki, K.; Galla, H.-J.; Wegener, J., Bioelectrical impedance assay to monitor changes in cell shape during apoptosis. *Biosensors and Bioelectronics* 2004, 19 (6), 583-594.
16. Singla, A. K.; Garg, A.; Aggarwal, D., Paclitaxel and its formulations. *International Journal of Pharmaceutics* 2002, 235 (1-2), 179-192.